

*The systems maintaining thermal regimes are a necessary component of thermally-loaded radio-electronic equipment, without which its operation is impossible. The uneven distribution of heat emitted by components such as semiconductor lasers, receivers of intense infrared radiation predetermines the preference of thermoelectric coolers for them. The joint application of a cooler and a heat-loaded element significantly tightens the requirements for the reliability indicators and the dynamic characteristics of the cooler. The cause is the influence exerted by the temperature gradients in the soldered joints between different materials of thermoelements and the electrode of the substrate. The main parameters of thermoelectric coolers are the number of thermoelements and the value of the working current. When targeting the design of thermoelectric systems for ensuring thermal regimes based on reliability indicators, the optimization of the problem for the following set has been proposed: the number of thermoelements, the working current, and the relative intensity of failures. At the fixed branches' geometry, decreasing the number of thermoelements leads to a decrease in the heat load, which can be compensated for by increasing the working current of the thermoelectric cooler. A ratio has been derived for the relative working current corresponding to the minimum size of the set. Using the set makes it possible to choose the required working current, for which there is an extremum, which optimizes the process of control over the cooler. The win in the refrigeration factor, compared to the mode of maximum cooling capacity, is 15 %. This demonstrates the advantage of a comprehensive indicator, which allows the development of systems enabling thermal modes for practical application, in particular, on-board systems for which energy consumption is critical. The originality of the results obtained is related to a comprehensive criterion for the basic performance indicators, which has a minimum*

**Keywords:** thermoelectric cooler, thermoelements, working current, failure rate, time to enter a mode

Received date 03.09.2020

Accepted date 09.10.2020

Published date 23.10.2020

## 1. Introduction

Among the basic parameters in designing the thermoelectric cooling devices (TCDs) are the number of thermoelements  $n$ , the value of the working current  $I$ , and the relative failure rate  $\lambda/\lambda_0$  at the fixed geometry of the thermoelements' branches (the ratio of thermoelement height to the area of its cross-section  $l/S$ ). For the rational construction of TCD, one should strive to reduce the number of thermoelements  $n$ , the value of the working current  $I$ , and the relative failure intensity  $\lambda/\lambda_0$ .

With the optimal design of TCD at the predefined geometry of the thermoelements' branches [1]:

- reducing the number of thermoelements  $n$  leads, on the one hand, to a decrease in the specified cooling capacity  $Q_0$  (the predefined heat load  $Q_0$ ) and the relative failure intensity  $\lambda/\lambda_0$ . This can be compensated for by an increase in the

# DEVELOPING A MODEL TO CONTROL THE THERMAL MODE OF THERMOELECTRIC COOLING DEVICES BY MINIMIZING THE SET OF THREE BASIC PARAMETERS

**V. Zaykov**

PhD, Head of Sector  
Research Institute «STORM»  
Tereshkovoi str., 27, Odessa, Ukraine, 65076  
E-mail: gradan@i.ua

**V. Mescheryakov**

Doctor of Technical Sciences, Professor, Head of Department  
Department of Informatics  
Odessa State Environmental University  
Lvivska str., 15, Odessa, Ukraine, 65016  
E-mail: gradan@ua.fm

**Yu. Zhuravlov**

PhD, Associate Professor  
Department of Technology of Materials and Ship Repair  
National University «Odessa Maritime Academy»  
Didrikhsona str., 8, Odessa, Ukraine, 65029  
E-mail: ivanovich1zh@gmail.com

Copyright © 2020, V. Zaykov, V. Mescheryakov, Yu. Zhuravlov

This is an open access article under the CC BY license

(http://creativecommons.org/licenses/by/4.0)

relative working current  $B$  but the relative failure rate  $\lambda/\lambda_0$  is also increasing in this case;

- decreasing the value of the working current  $I$  leads to a decrease in the cooling capacity  $Q_0$  (the predefined heat load  $Q_0$ ), which can be compensated for by increasing the number of thermoelements  $n$ .

- the decrease in the relative failure intensity  $\lambda/\lambda_0$  is associated with a decrease in the number of thermoelements  $n$  and the value of the working current  $I$ .

Thus, the set of basic parameters  $(n, I, \lambda/\lambda_0)_{\min}$  is interconnected; potentially, there is an optimal relative working current  $B_{opt}$ , corresponding to the minimum magnitude of the set  $(n, I, \lambda/\lambda_0)_{\min}$ .

The use of thermoelectric coolers as active systems to maintain heat modes for the thermally-loaded elements makes it possible to adapt to heat load quickly. This approach helps reduce the temperature gradients in the interconnect-

ed thermally-loaded element and the means of heat selection and, as a result, improve the reliability indicators of critical systems. However, the cooler operational conditions become stricter in this case due to the need for the growth of the dynamic characteristics and the increase in the temperature gradients in the soldered joints between the thermoelements and electrodes. This renders relevance to research aimed at improving the dynamic performance, reliability indicators, and ways to manage the operational modes of thermoelectric coolers that take these indicators into consideration.

## 2. Literature review and problem statement

Work [2] considers issues relating to providing thermal modes for heat-loaded equipment and shows that the distribution of heat load is heterogeneous while the volumetric cooling of electronic units is not effective. A significant difference in the density of heat-emitting sources such as semiconductor lasers, receivers of intense radiation makes the local heat selection systems preferable, which are subject to additional requirements for the dynamics and reliability indicators [3]. The cited work demonstrates that from the standpoint of reliability theory, the heat-loaded element and the means of heat selection are enabled sequentially with the resulting probability of failure-free operation equal to the product of probabilities of the components. However, the alignment of thermal mode systems with the requirements for the mass-dimension characteristics of on-board systems was not considered. In terms of weight, size, and dynamic characteristics, there is currently no alternative to thermoelectric cooling devices [4]. The ability to remove heat is influenced by the energy relationship between the heat-loaded element and the cooler, which is considered in paper [5]. The analysis was carried out for static modes, which solves only part of the problem of the cooler interaction with the load. Further research was aimed at taking into consideration stricter operating conditions and improving the reliability indicators of thermoelectric coolers at all stages of their life cycle [6]. Taking into consideration the impact of the design parameters of thermoelectric coolers and the structural integrity of their modules on reliability indicators has made it possible to optimize the performance of the device under a static mode [7]. Subsequent studies were aimed at analyzing the dynamic characteristics of thermoelectric coolers as the increase in the temperature gradient in the soldered joint between the thermoelement and electrode leads to an increase in temperature stresses and a decrease in reliability [8]. The contradiction between the dynamics and reliability is a fundamental issue and is used for the accelerated testing of thermoelectric coolers for reliability at the cyclical change in the polarity of the power, at which reliability indicators fall by an order of magnitude [9]. Control mode renders the dynamic characteristics of the thermoelectric cooler important as they exert a direct impact on reliability indicators. An analysis of the relationship between the dynamic characteristics of thermoelements and reliability indicators is reported in work [10], which explores the impact of energy indicators in the working range of thermoelectric cooler operation. The issues of the impact exerted by the structural and technological parameters on the reliability indicators and dynamic characteristics of the thermoelectric cooler in the working range of current modes and temperature changes, addressed in work [11], remained unexplored. An analysis of the effect of the physical parameters of thermoelement materials on the reliability indicators and dynamic characteristics of the thermoelectric

cooler was performed in paper [12], where it was shown that the varying electrical conductivity could achieve the improvement of these indicators. The reported study is aimed at analyzing the effect of a single indicator or parameter on the reliability and dynamics of the cooler. At the same time, it is important for control tasks to consider a significant set of indicators that would allow for the optimized design of thermal mode systems on thermoelectric coolers.

## 3. The aim and objectives of the study

The aim of this work is to determine, for the relative working current, the optimal value of the minimum set of the product of the number of thermoelements, working current, and the relative failure intensity, which would make it possible to minimize the relative working current to control the thermoelectric cooler.

To accomplish the aim, the following tasks have been set:

- to develop an analytical model of the set's relation to the energy indicators of the thermoelectric cooler;
- to analyze the relationship between the working current and the number and geometry of thermoelements, as well as the time to enter a stationary mode.

## 4. Developing an analytical model of the set's relation to the energy indicators of the thermoelectric cooler

The number of thermoelements  $n$  in a single-cascade thermoelectric cooler can be determined from the ratio given in [1]:

$$n = \frac{Q_0}{I_{\max K}^2 R_K (2B_K - B_K^2 - \Theta)}, \quad (1)$$

where  $Q_0$  is the value of heat load is, W;

$$I_{\max K} = \frac{\bar{e}_K T_0}{R_K} \text{ is the maximum working current, A.}$$

$\bar{e}_K$  is the averaged value of the thermo EMF coefficient of a thermoelement's branch at the end of the cooling process, W/K;

$R_K = \frac{l}{\bar{\sigma}_K S}$  is the electrical resistance of a thermoelement's branch, Ohm;

$l$  and  $S$  are, respectively, the height  $l$  and the area of the cross-section  $S$  of a thermoelement's branch;

$\bar{\sigma}_K$  is the averaged value of the electroconductivity of a thermoelement's branch, Sm/cm;

$T_c$  is the temperature of a heat-absorbing soldered joint, K;

$B_K = \frac{I}{I_{\max K}}$  is the relative working current at the end of the cooling process;  $\Theta = \frac{T - T_0}{\Delta T_{\max}}$  is the relative temperature difference;

$T$  is the temperature of a heat-emitting soldered joint, K;

$\Delta T_{\max} = 0.5 \bar{z} T_0^2$  is the maximum temperature difference, K;

$\bar{z}$  is the averaged efficiency of the stating thermoelectric materials in a module, 1/K.

The TCD consumed power  $W_K$  can be determined from the following expression:

$$W_K = 2n \cdot I_{\max K}^2 \cdot R_K \cdot B_K \left( B_K + \frac{\Delta T_{\max}}{T_0} \Theta \right). \quad (2)$$

The voltage drop  $U_K$

$$U_K = \frac{W_K}{I}. \quad (3)$$

The refrigeration factor  $E$  can be calculated from the following expression:

$$E = \frac{Q_0}{W_K}. \quad (4)$$

The relative value of failure intensity  $\lambda/\lambda_0$  can be determined from the expression given in [1]:

$$\lambda/\lambda_0 = nB_K^2(\Theta + C) \frac{\left(B_K + \frac{\Delta T_{\max}}{T_0} \Theta\right)^2}{\left(1 + \frac{\Delta T_{\max}}{T_0} \Theta\right)^2} \cdot K_T, \quad (5)$$

where  $C = \frac{Q_0}{nI_{\max K}^2 R_K}$  is the relative heat load;  $K_T$  is the significant factor of lower temperatures.

The probability of a TCD failure-free operation  $P$  can be determined from the following expression:

$$P = \exp[-\lambda t], \quad (6)$$

where  $t$  is the designated resource, h.

A ratio for determining the time to enter a stationary operation mode  $\tau$  [10] can be represented in the following form:

$$\tau = \frac{\sum_i m_i C_i}{K_K \left(1 + 2B_K \frac{\Delta T_{\max}}{T_0}\right)} \ln \frac{\gamma B_H (2 - B_H)}{2B_K - B_K^2 - \Theta}, \quad (7)$$

where  $\gamma = \frac{I_{\max H}^2 R_H}{I_{\max K}^2 R_K}$ ;

$\sum_i m_i C_i$  is the total value of the product of heat capacity

and the mass of components of the structural and technological elements (STE) on the heat-absorbing soldered joint in a module at the set ratio  $l/S$ ;

$R_H$  is the electrical resistance of a thermoelement's branch at the beginning of the cooling process, Ohm;

$B_H = \frac{I}{I_{\max H}}$  is the relative working current at  $\tau=0$  at the beginning of the cooling process;

$I_{\max H} = \frac{e_H \cdot T}{R_H}$  is the maximum working current at the beginning of the cooling process, A.

Subject to equal currents at the beginning and end of the cooling process:

$$I = B_K I_{\max K} = B_H I_{\max H}.$$

Then an expression for the set  $(n, I, \lambda/\lambda_0)$  can be written in the following form:

$$K = nI\lambda/\lambda_0 = \frac{Q_0^2 I_{\max} B^3 (\Theta + C) \left(B + \frac{\Delta T_{\max}}{T_0} \Theta\right)^2 K_T}{I_{\max}^4 R^2 (2B - B^2 - \Theta)^2 \left(1 + \frac{\Delta T_{\max}}{T_0} \Theta\right)^2}, \quad (8)$$

or in the form suitable for differentiating:

$$A = \frac{KI_{\max}^3 R^2 \left(1 + \frac{\Delta T_{\max}}{T_0} \Theta\right)^2}{Q_0^2 K_T (\Theta + C)} = \frac{B^3 \left(B + \frac{\Delta T_{\max}}{T_0} \Theta\right)^2}{(2B - B^2 - \Theta)^2}, \quad (9)$$

The condition  $\frac{dA}{dB} = 0$  is used to derive ratios for determining the optimal value of the relative working current  $B_{opt}$ , corresponding to the minimum value of the  $(nI\lambda/\lambda_0)_{\min}$  set:

$$B_{opt}^3 - B_{opt}^2 \left(6 + \frac{\Delta T_{\max}}{T_0} \Theta\right) - B_{opt} \Theta \left(5 - 2 \frac{\Delta T_{\max}}{T_0}\right) + 3 \frac{\Delta T_{\max}}{T_0} \Theta^2 = 0. \quad (10)$$

The resulting expressions link the dynamic and reliability characteristics with the energy indicators and design parameters of thermoelectric coolers in the working range of operation while the introduction of the set contributes to the optimized control over a system that manages thermal regimes.

### 5. Analysis of the analytical model of the set's relationship with the energy indicators of the thermoelectric cooler

The results of calculating a functional dependence  $\lambda=f(B)$  for different temperature drops  $\Theta$  depending on the relative working current  $B$  are shown in Fig. 1.

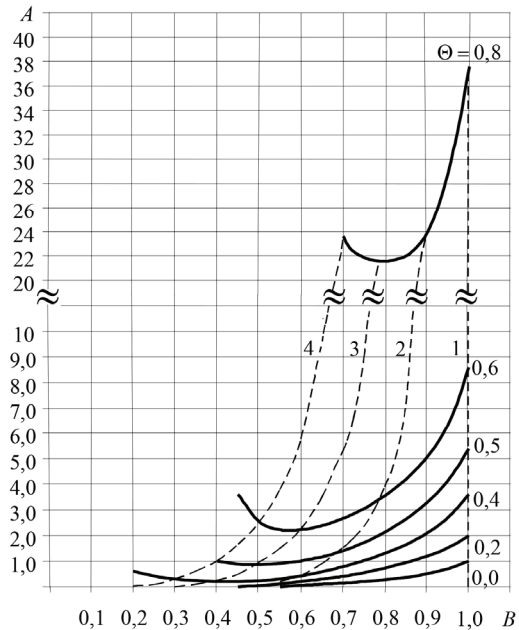


Fig. 1. Dependence of the value

$$nI\lambda/\lambda_0 I_{\max}^3 R^2 \left(1 + \frac{\Delta T_{\max}}{T_0} \Theta\right)^2$$

$$A = \frac{Q_0^2 K_T (\Theta + C)}{Q_0^2 K_T (\Theta + C)}$$

in a single-cascade TCD on the relative working current  $B$  for various relative temperature drops  $\Theta$  at  $T=300$  K,  $Q_0=0.5$  W,  $l/S=4.5$ ; 1 -  $Q_{0\max}$  mode; 2 -  $(n, I)_{\min}$  mode; 3 -  $(nI\lambda/\lambda_{00})_{\min}$  mode; 4 -  $\lambda_{\min}$  mode

The functional dependence of the set  $\lambda=f(B)$  (Fig. 1) has a minimum for different relative temperature drops  $\Theta$  at  $T=300$  K and heat load  $Q_0=0.5$  W. For example, at  $\Theta=0.5$ , the magnitude  $A=0.83$  at  $B_{opt}=10.47$  under the  $(nI\lambda/\lambda_0)_{min}$  mode.

As the relative temperature difference  $\Theta$  increases, the value of the set  $A$  increases.

Dotted line indicates a geometric location of points corresponding to different current operational modes: 1 –  $Q_{0max}$  mode; 2 –  $(n, I)_{min}$  mode; 3 –  $(nI\lambda/\lambda_0)_{min}$  mode; 4 –  $\lambda_{min}$  mode.

Fig. 2 shows the dependence of the set  $A$  on the relative temperature difference  $\Theta$  for different current modes of operation.

The minimum value of the  $(nI\lambda/\lambda_0)_{min}$  set corresponds to the  $(nI\lambda/\lambda_0)_{min}$  mode and:

- at  $\Theta=0.5$ , it is  $A=0.831$  under the  $(nI\lambda/\lambda_0)_{min}$  mode;
- at  $\Theta=0.5$ , it is  $A=0.987$  under the  $\lambda_{min}$  mode;
- at  $\Theta=0.5$ , it is  $A=1.48$  under the  $(nI)_{min}$  mode;
- at  $\Theta=0.5$ , it is  $A=5.29$  under the  $Q_{0max}$  mode.

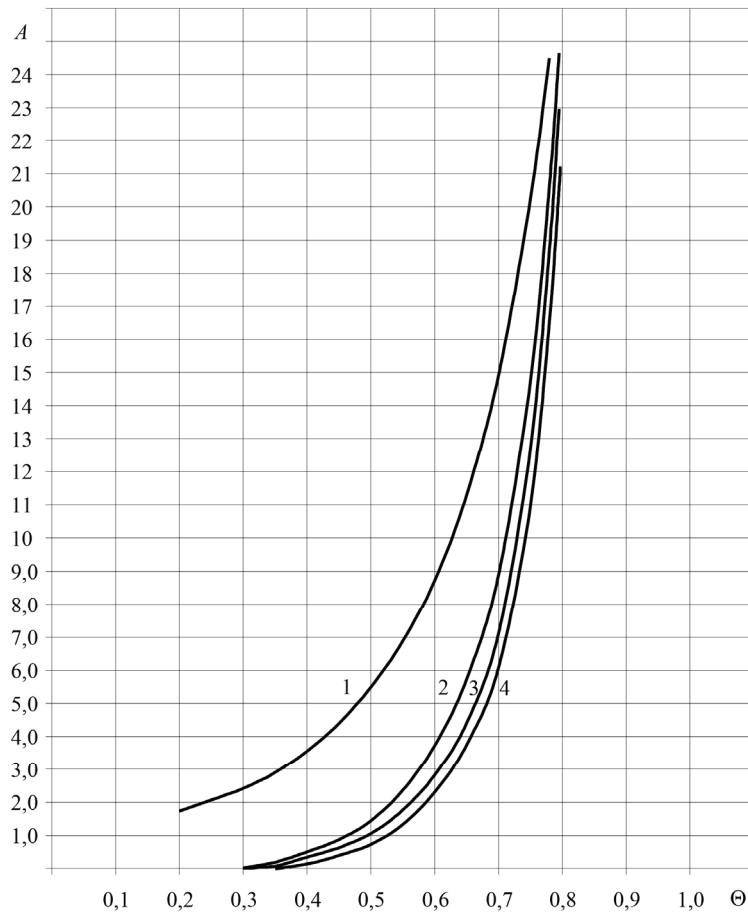


Fig. 2. Dependence of the value  $A$  for a single-cascade TCD on the relative temperature difference  $\Theta$  for the various modes of operation at  $T=300$  K,  $Q_0=0.5$  W,  $l/S=4.5$ ; 1 –  $Q_{0max}$  mode; 2 –  $(n, I)_{min}$  mode; 3 –  $\lambda_{min}$  mode; 4 –  $(n, I, \lambda/\lambda_0)_{min}$  mode

The results of calculating the basic parameters, reliability indicators, and the time to enter the stationary mode of operation by a single-cascade TCD at  $T=300$  K, temperature difference  $\Delta T=40$  K, heat load  $Q_0=0.5$  W, and the geometry of the thermoelements' branches (the ratio  $l/S=4.5$ ; 10; 20; 40), are given in Table 1.

Increasing the relative working current  $B$  at temperature difference  $\Delta T=40$  K and heat load  $Q_0=0.5$  W for different ge-

ometry of the thermoelements' branches (the ratio  $l/S=4.5$ ; 10; 20; 40) leads to the following:

- the number of thermoelements  $n$  decreases (Fig. 3). As the  $l/S$  ratio grows, the number of thermoelements  $n$  increases at the fixed relative working current  $B$ ;

- the value of the working current  $I$  increases (Fig. 4). As the  $l/S$  ratio grows, the value of the working current  $I$  decreases at the fixed relative working current;

- the functional dependence of the  $(n, I, \lambda/\lambda_0)=f(B)$  set on the relative working current  $B$  has a minimum at  $B=0.47$  for different geometry of the thermoelements' branches  $l/S$ . With the growth of the  $l/S$  ratio, the value of the set increases at the fixed relative working current  $B$  (Fig. 5);

- the functional dependence of voltage drop  $U=f(B)$  on the relative working current  $B$  has a minimum at  $B=0.71$  under the  $(n, I)_{min}$  mode. With the growth of the  $l/S$  ratio, the voltage drop value  $U$  increases at the fixed relative working current  $B$  (Fig. 6);

- the functional dependence of the refrigeration factor  $E=f(B)$  on the relative working current  $B$  has a maximum at  $B=0.53$  under the  $E_{min}$  mode (Fig. 6). The refrigeration factor  $E$  does not depend on the geometry of the thermoelements' branches ( $l/S$  ratio);

- the time to enter a stationary mode of operation  $\tau$  decreases (Fig. 7). As the  $l/S$  ratio grows, the time to enter a stationary mode of operation decreases at the fixed relative working current  $B$ ;

- the relative failure rate  $\lambda/\lambda_0$  increases (Fig. 8). As the  $l/S$  ratio increases, the relative failure rate increases at the fixed relative working current  $B$ ;

- the likelihood of failure-free operation  $P$  decreases (Fig. 8). As the  $l/S$  ratio grows, the probability of failure-free operation  $P$  decreases at the fixed relative working current  $B$ ;

- the functional dependence of the amount of energy spent  $N=f(B)$  on the relative working current  $B$  has a minimum at  $B=0.71$  under a mode of  $(n, I)_{min}$  for different geometry of the thermoelements' branches ( $l/S$  ratio) (Fig. 9). As the  $l/S$  ratio grows, the amount of energy spent  $N$  decreases at the fixed relative working current  $B$ .

The results of calculating the basic parameters, reliability indicators, and the time to enter a stationary mode of operation  $\tau$  are under the  $(n, I, \lambda/\lambda_0)_{min}$  mode for various temperature drops  $\Delta T$ , from  $\Delta T=10$  K to  $\Delta T=60$  K, for  $l/S=4.5$  are given in Table 2.

Increasing the temperature difference  $\Delta T$  under the mode of  $(n, I, \lambda/\lambda_0)_{min}$  at the heat load  $Q_0=0.5$  W and the ratio  $l/S=4.5$  leads to the following:

- the functional dependence of the number of thermoelements  $n=f(\Delta T)$  has a minimum at  $\Delta T=40$  K,  $n=4.1$  pcs. (Fig. 10, p. 1);

- the working current  $I$  increases (Fig. 10, p. 2);

- the refrigeration factor  $E$  decreases (Fig. 10, p. 3);

- the time to enter a stationary mode of operation  $\tau$  increases (Fig. 11, p. 1);

- the relative failure intensity increases,  $\lambda/\lambda_0$  (Fig. 11, p. 2);

- the likelihood of failure-free operation  $P$  decreases (Fig. 11, p. 3);

- the voltage drop  $U$  increases (Fig. 12, p. 1);

- the amount of energy spent  $N$  increases (Fig. 12, p. 2).

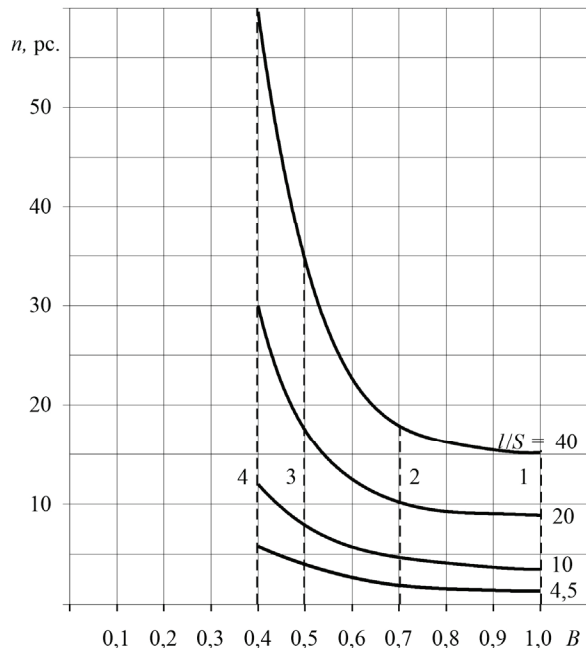


Fig. 3. Dependence of the number of thermoelements  $n$  in a single-cascade TCD on the relative working current  $B$  for different geometry of the thermoelements' branches  $l/S$  at  $T=300$  K,  $Q_0=0.5$  W,  $\Delta T=40$  K; 1 –  $Q_{0max}$  mode; 2 –  $(n\eta)_{min}$  mode; 3 –  $(n, I, \lambda/\lambda_0)_{min}$  mode; 4 –  $\lambda_{min}$  mode

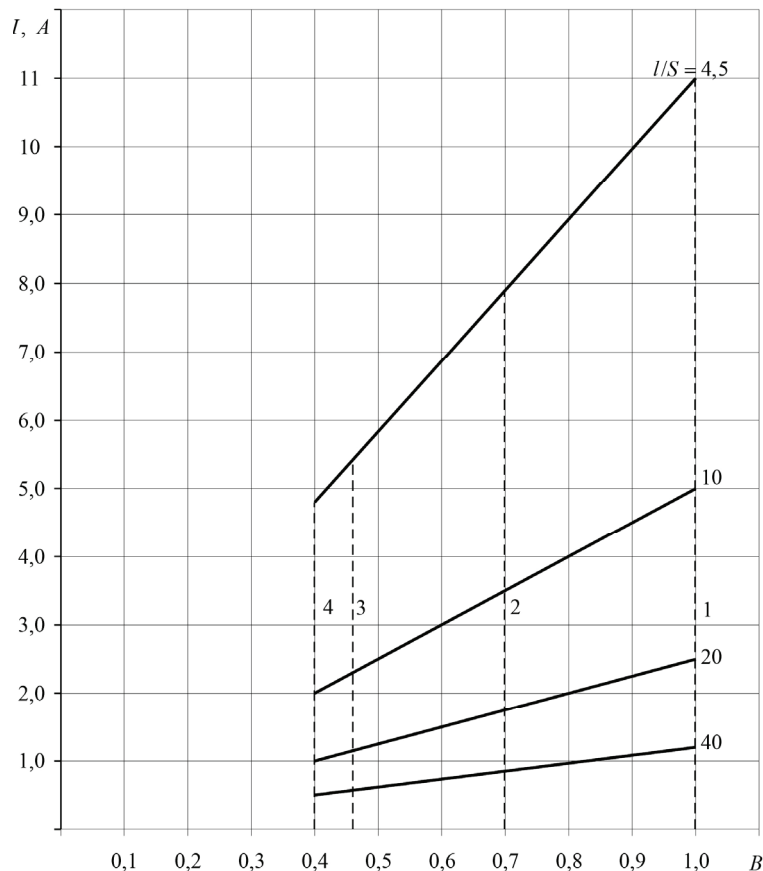


Fig. 4. Dependence of the value of working current  $I$  in a single-cascade TCD on the relative working current  $B$  for different geometry of the thermoelements' branches ( $l/S$  ratio) at  $T=300$  K,  $\Delta T=40$  K,  $Q_0=0.5$  W: 1 –  $Q_{0max}$  mode; 2 –  $(n\eta)_{min}$  mode; 3 –  $(n, I, \lambda/\lambda_0)_{min}$  mode; 4 –  $\lambda_{min}$  mode

The resulting relationship between the dynamics of the functioning and energy characteristics of a single-cascade thermoelectric cooler under the  $(n, I, \lambda/\lambda_0)_{min}$  mode

on the temperature difference makes it possible to choose the design conditions that best satisfy the problem considered.

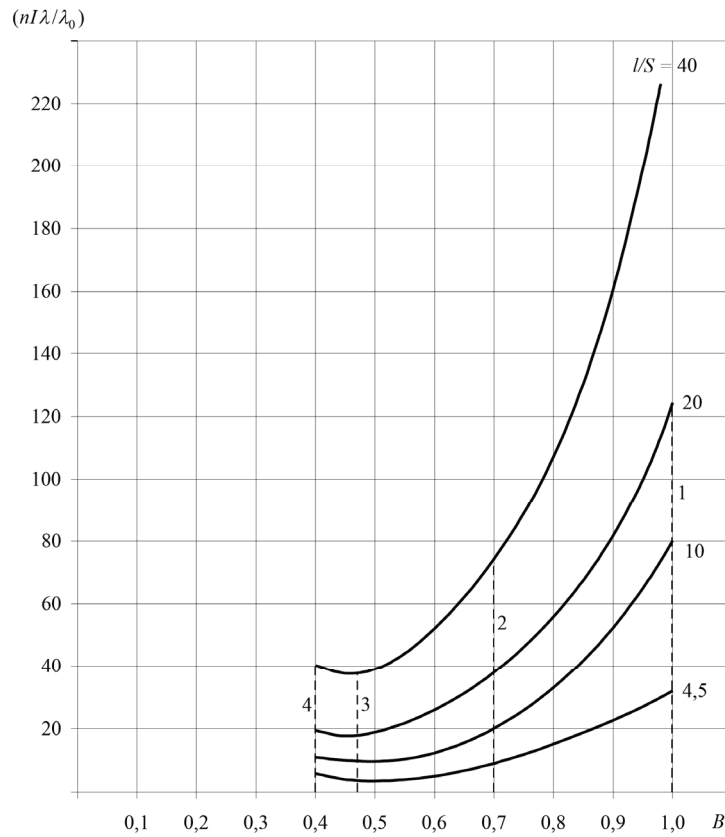


Fig. 5. Dependence of the  $(n, I, \lambda/\lambda_0)$  in a single-cascade TCD on the relative working current  $B$  for various  $I/S$  at  $T=300$  K,  $\Delta T=40$  K,  $Q_0=0.5$  W; 1 –  $Q_{0max,x}$  mode; 2 –  $(nI)_{min}$  mode; 3 –  $(n, I, \lambda/\lambda_0)_{min}$  mode; 4 –  $\lambda_{min}$  mode

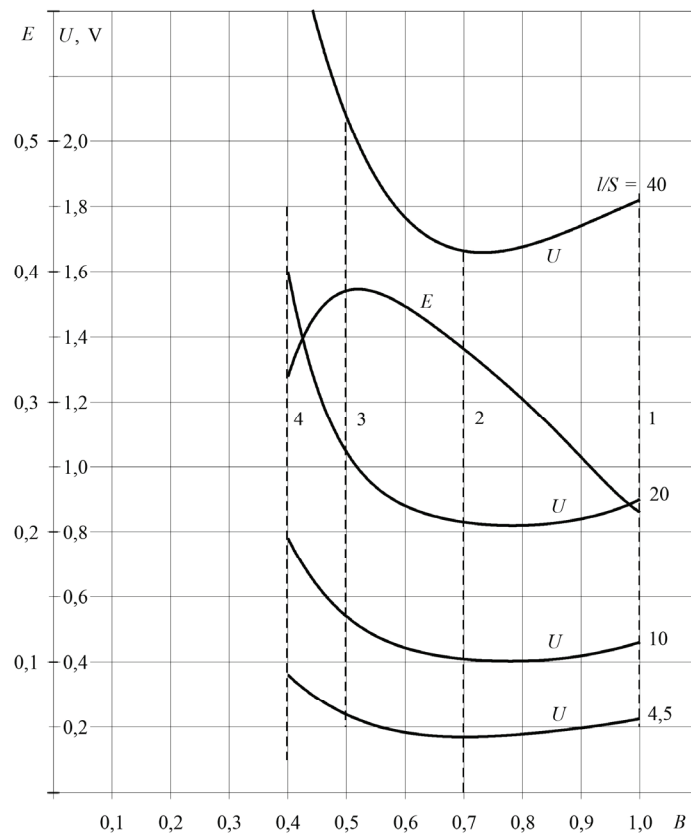


Fig. 6. Dependence of the refrigeration factor  $E$ , the voltage drop  $U$  in a single-cascade TCD on the relative working current  $B$  for different geometry of the thermoelements' branches  $I/S$  at  $T=300$  K,  $\Delta T=40$  K,  $Q_0=0.5$  W; 1 –  $Q_{0max,x}$  mode; 2 –  $(nI)_{min}$  mode; 3 –  $(n, I, \lambda/\lambda_0)_{min}$  mode; 4 –  $\lambda_{min}$  mode



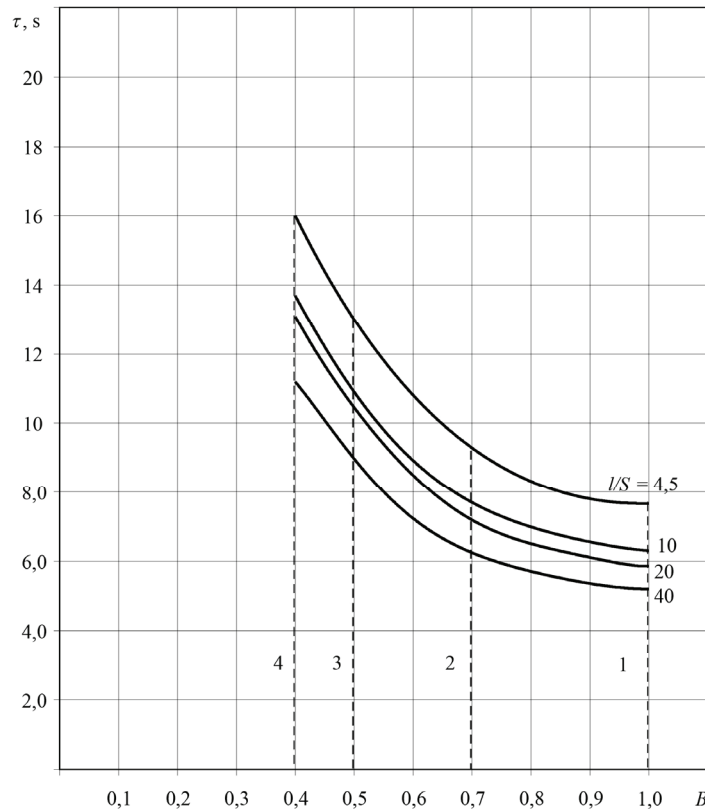


Fig. 7. Dependence of the time to enter a stationary mode of operation  $\tau$  by a single-cascade TCD on the relative working current  $B$  for different geometry of the thermoelements' branches  $l/S$  at  $T=300$  K,  $Q_0=0.5$  W,  $\Delta T=40$  K; 1 –  $Q_{0max}$  mode; 2 –  $(nl)_{min}$  mode; 3 –  $(n, l, \lambda/\lambda_0)_{min}$  mode; 4 –  $\lambda_{min}$  mode

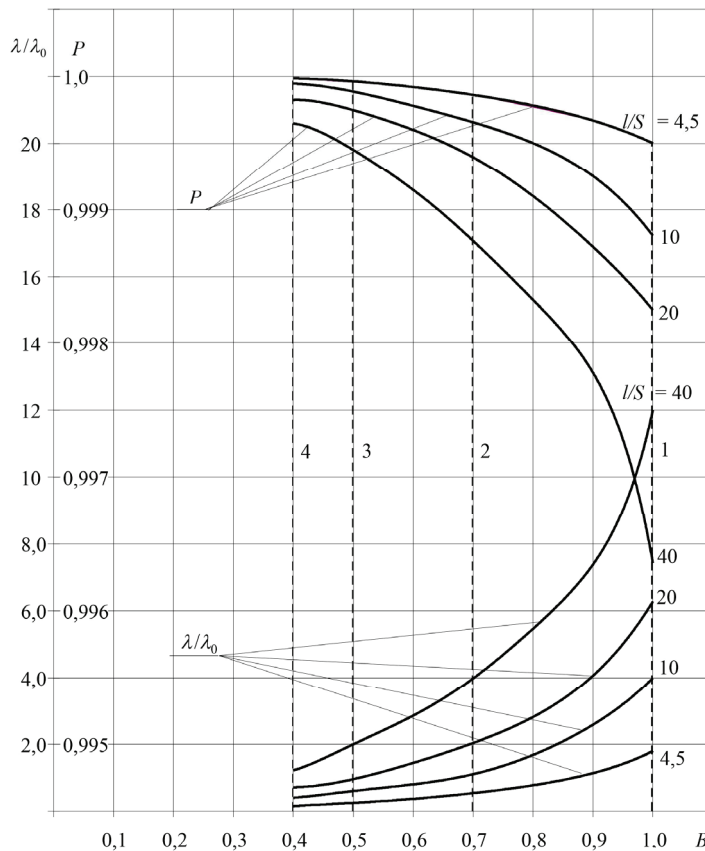


Fig. 8. Dependence of the relative failure intensity  $\lambda/\lambda_0$  and the probability of failure-free operation  $P$  by a single-cascade TCD on the relative working current  $B$  for different geometry of the thermoelements' branches ( $l/S$ ) at  $T=300$  K;  $Q_0=0.5$  W;  $\Delta T=40$  K; 1 –  $Q_{0max}$  mode; 2 –  $(nl)_{min}$  mode; 3 –  $(n, l, \lambda/\lambda_0)_{min}$  mode; 4 –  $\lambda_{min}$  mode

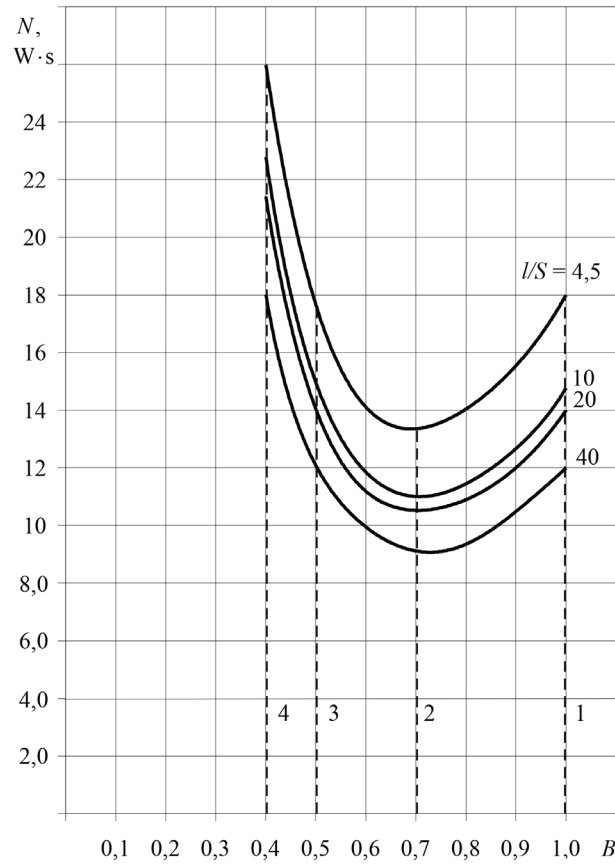


Fig. 9. Dependence of the amount of energy spent  $N$  by a single-cascade TCD on the relative working current  $B$  for different geometry of the thermoelements' branches  $l/S$  at  $T=300$  K;  $\Delta T=40$  K;  $Q_0=0.5$  W;  
 1 –  $Q_{0max}$  mode; 2 –  $(n\eta)_{min}$  mode; 3 –  $(n, I, \lambda/\lambda_0)_{min}$  mode; 4 –  $\lambda_{min}$  mode

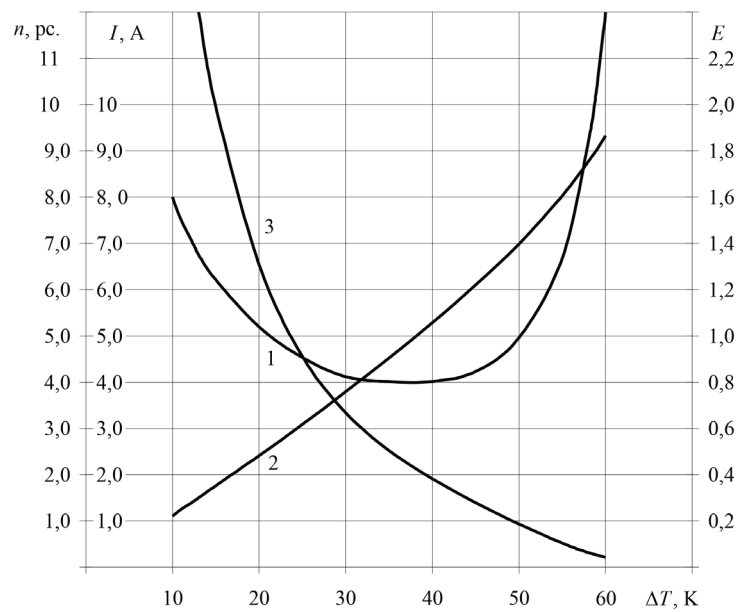


Fig. 10. Dependence of the number of thermoelements  $n$ , the value of the working current  $I$ , the refrigeration factor  $E$  on the temperature difference  $\Delta T$  under the mode of  $(n, I, \lambda/\lambda_0)_{min}$  at  $T=300$  K;  $Q_0=0.5$  W;  $l/S=4.5$ ; 1 –  $n=f(\Delta T)$ ; 2 –  $I=f(\Delta T)$ ; 3 –  $E=f(\Delta T)$



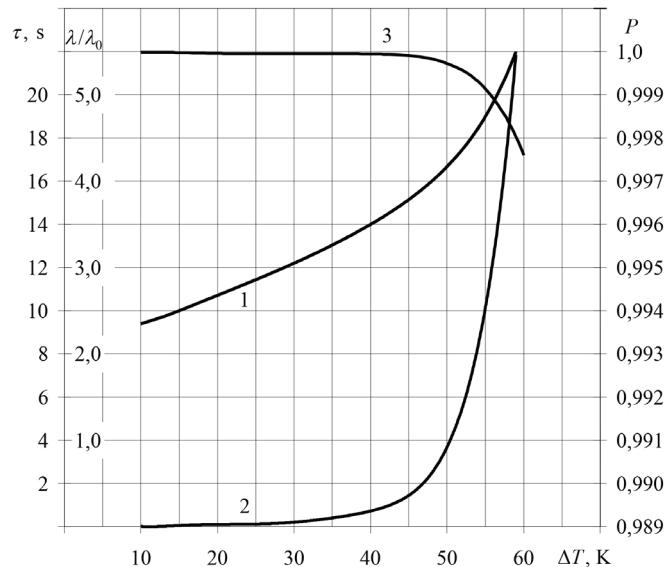


Fig. 11. Dependence of the time to enter a stationary mode of operation  $\tau$ , the relative failure intensity  $\lambda/\lambda_0$ , and the probability of failure-free operation  $P$  by a single-cascade TCD on the temperature difference  $\Delta T$  at  $T=300$  K;  $Q_0=0.5$  W;  $I/S=4.5$ ; 1 –  $\tau=f(\Delta T)$ ; 2 –  $\lambda/\lambda_0=f(\Delta T)$ ; 3 –  $P=f(\Delta T)$

Table 1

Results of calculating the TCD basic parameters at  $T=300$  K;  $\Delta T=40$  K;  $\Delta T_{max}=79.8$  K;  $\Theta=0.5$ ;  $Q_0=0.5$  W

I/S	Mode of operation	B	$R \cdot 10^3$ , Ohm	$I_{max}$ , A	n, pc.	W, W	U, V	E	I, A	nI	$nI/\lambda_0$	$\tau$ , s	N, W·s	$\lambda/\lambda_0$	$\lambda \cdot 10^8$ , 1/h	P	
4.5	$Q_{0min}$	1.0	4.55	11.1	1 1.8	2.32	0.21	0.22	11.1	20.0	32.0	7.8	17.9	1.6	4.8	0.99955	
	$(nI)_{min}$	0.71			2.3	1.46	0.19	0.34	8.0	16.9	7.4	9.2	13.4	13.4	0.44	1.53	0.99985
	$(nI/\lambda_0)_{min}$	0.47			4.1	1.35	0.26	0.37	5.2	21.3	4.11	13.9	18.8	0.193	0.58	0.999942	
	$\lambda_{min}$	0.40			6.6	1.62	0.34	0.31	4.8	31.7	4.9	16.0	25.9	0.154	0.462	0.999954	
10	$Q_{0max}$	1.0	10.1	5.02	3.9	2.30	0.46	0.22	5.02	19.6	78.3	6.4	14.7	4.0	12.0	0.99880	
	$(nI)_{min}$	0.71			4.75	1.463	0.41	0.34	3.55	16.9	20.7	7.7	11.2	1.23	3.7	0.99963	
	$(nI/\lambda_0)_{min}$	0.47			9.0	1.345	0.57	0.37	2.36	21.2	9.0	12.0	16.1	0.424	1.27	0.99987	
	$\lambda_{min}$	0.40			15.0	1.62	0.81	0.31	2.0	24.0	10.8	14.0	22.7	0.36	1.1	0.99990	
20	$Q_{0max}$	1.0	20.2	2.51	7.9	2.32	0.92	0.22	2.51	19.8	122.9	6.0	13.8	6.2	18.5	0.9982	
	$(nI)_{min}$	0.71			10.3	1.46	0.81	0.34	1.80	18.5	37.1	7.4	10.8	2.0	6.0	0.99941	
	$(nI/\lambda_0)_{min}$	0.47			17.9	1.33	1.18	0.37	1.18	21.1	17.8	11.7	15.6	0.845	2.53	0.99975	
	$\lambda_{min}$	0.40			29.3	1.62	1.61	0.31	1.0	29.3	19.7	13.3	21.5	0.673	2.02	0.99980	
40	$Q_{0max}$	1.0	40.4	1.255	16.0	2.32	1.83	0.22	1.255	20.1	245.2	5.2	12.0	12.2	36.7	0.9963	
	$(nI)_{min}$	0.71			20.8	1.46	1.65	0.34	0.89	18.5	74.0	6.3	9.2	4.0	12.0	0.9988	
	$(nI/\lambda_0)_{min}$	0.47			35.9	1.33	2.26	0.37	0.59	21.2	35.8	10.5	14.0	1.69	5.08	0.99949	
	$\lambda_{min}$	0.40			59.6	1.62	3.1	0.31	0.53	31.6	42.3	11.2	18.1	1.36	4.0	0.99960	

Table 2

Results of calculating the TCD basic parameters under the  $(nI/\lambda_0)_{min}$  mode at  $T=300$  K;  $Q_0=0.5$  W;  $I/S=4.5$ ;  $R_{\mu}=5 \cdot 10^{-3}$  Ohm;  $I_{max}=12.24$  A

B	n, pc.	I, A	U, V	E	W, W	$\tau$ , s	N, W·s	$\alpha F$ , W/K	$\lambda/\lambda_0$	$\lambda \cdot 10^8$ 1/h	P
$\Delta T=10$ K, $T_0=290$ K, $\Delta T_{max}=101$ K; $\Theta=0.1$ ; $R=4.89 \cdot 10^{-3}$ Ohm; $I_{min}=12.0$ A											
0.10	7.9	1.2	0.125	3.33	0.15	9.6	1.4	0.13	0.00255	0.00077	0.99999924
$\Delta T=20$ K, $T_0=280$ K, $\Delta T_{max}=93.7$ K; $\Theta=0.213$ ; $R=4.74 \cdot 10^{-3}$ Ohm; $I_{min}=11.83$ A											
0.20	5.1	2.36	0.154	1.37	0.36	11.3	4.1	0.17	0.00475	0.0142	0.9999986
$\Delta T=30$ K, $T_0=270$ K, $\Delta T_{max}=86.8$ K; $\Theta=0.346$ ; $R=4.69 \cdot 10^{-3}$ Ohm; $I_{min}=11.46$ A											
0.32	4.2	3.67	0.19	0.70	0.71	12.5	8.9	0.24	0.0355	0.107	0.999989
$\Delta T=40$ K, $T_0=260$ K, $\Delta T_{max}=79.8$ K; $\Theta=0.50$ ; $R=4.55 \cdot 10^{-3}$ Ohm; $I_{min}=11.1$ A											
0.47	4.1	5.2	0.26	0.37	1.35	13.9	18.8	0.37	0.195	0.584	0.999942
$\Delta T=40$ K, $T_0=260$ K, $\Delta T_{max}=79.8$ K; $\Theta=0.50$ ; $R=4.55 \cdot 10^{-3}$ Ohm; $I_{min}=11.1$ A											
$\Delta T=50$ K, $T_0=250$ K, $\Delta T_{max}=73.1$ K; $\Theta=0.684$ ; $R=4.41 \cdot 10^{-3}$ Ohm; $I_{min}=10.9$ A											
0.655	4.8	7.14	0.39	0.178	2.81	16.4	46.1	0.66	0.947	2.84	0.99972
$\Delta T=60$ K, $T_0=240$ K, $\Delta T_{max}=66.8$ K; $\Theta=0.90$ ; $R=4.33 \cdot 10^{-3}$ Ohm; $I_{min}=10.53$ A											
0.885	12.0	9.32	1.24	0.043	11.6	23.6	274	2.42	7.92	23.8	0.9976

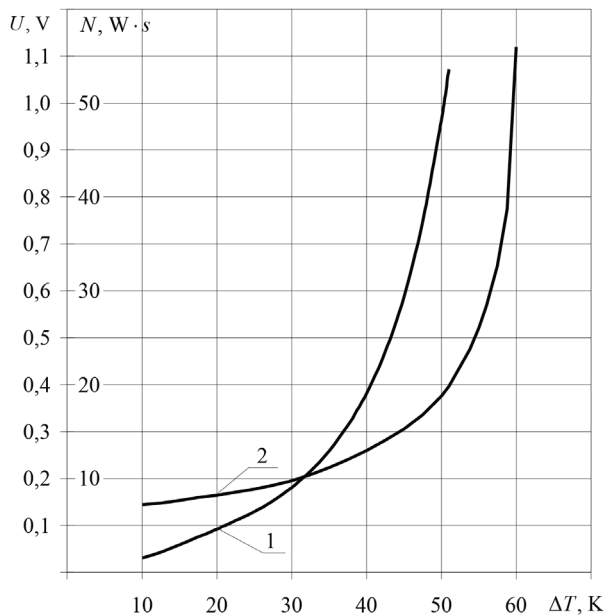


Fig. 12. Dependence of the voltage drop  $U$  and the amount of energy spent  $N$  by a single-cascade TCD on temperature change  $\Delta T$  at  $T=300$  K;  $Q_0=0.5$  W;  $l/S=4.5$ ; 1 –  $U=f(\Delta T)$ ; 2 –  $N=f(\Delta T)$

## 6. Discussion of results of studying a model of the set's relationship to the energy characteristics of the thermoelectric cooler

We have analyzed the analytical model of the set's relationship with the working current, heat load, temperature difference, the resistance of a thermoelement in the working range of temperature changes, and the geometry of the thermoelements. The model takes into consideration the pattern in managing complex objects whereby the set of indicators consisting of the number of thermoelements, the working current, and the relative failure intensity better fits the requirements for optimizing the control over a thermoelectric cooler. As our analysis of the scientific literature has revealed, the issue of optimization efficiency based on a single indicator is limited by that all the indicators in a thermoelectric device are interconnected. Reducing the number of thermoelements leads to a decrease in the failure rate and reduced cooling capacity, whose restoration requires an increase in the working current, which increases the failure rate. It has been shown that the use of the set makes it possible to choose the required working current, for which there is an extremum (Fig. 5), which optimizes the process of control over a cooler. The win in the refrigeration factor under the mode of  $(n, I, \lambda/\lambda_0)_{\min}$  is, compared to the  $Q_{0\max}$  mode, 15 % (Fig. 6), which indicates the advantage of control when using an integrated indicator. The dependence of energy spent

on the relative working current at different geometry of the thermoelements has a pronounced minimum (Fig. 9), which makes it possible to design systems for enabling thermal modes at on-board applications, for which energy consumption is critical.

The practical significance of our study is evident in regard to the on-board systems for enabling thermal modes in radio electronic equipment, for which the indicators of cooling capacity, reliability, as well as the mass-size characteristics, are important. The need to reduce cooling capacity is due to the limited resource of on-board energy equipment while mass-size characteristics affect both the performance of heat-loaded components and the increase in the share of payload of the product. An integrated reliability indicator largely determines the functionality of the product in which the systems for enabling thermal modes are located because, if these indicators' values are not enough, the product turns out either almost useless or dangerous to apply.

The limitations of this study are mainly due to the prerequisites for building the model: the identity of the characteristics of all thermoelements, regardless of their location and the quality of thermal contacts, which does not take into consideration the boundary effects of heat transmission and manufacturing technology. If the distribution of heat flow at the surface of the thermoelectric cooler's electrode is significant, it would require a significant amount of research beyond the scope of our study. Further research involving the proposed models implies changing the components of the attribute set and expanding it relative to the objective function of the task.

## 8. Conclusions

1. We have developed an analytical model to determine the relative working current  $B_{opt}$  at minimizing the set  $(n, I, \lambda/\lambda_0)_{\min}$  for temperature changes from  $\Delta T=10$  K to  $\Delta T=60$  K at the heat load  $Q_0=0.5$  W, and the geometry of the thermoelements' branches  $l/S=4.5$ ; 10; 20; 40. The model links the dynamic and reliability characteristics with the energy and structural parameters of the thermoelectric cooler in the operational range and makes it possible to assess the impact of each component; it allows the optimized design of systems that enable thermal modes for thermoelectric coolers.

2. The analysis of the model produced an assessment of the basic parameters, the reliability and dynamic characteristics of single-cascade thermoelectric coolers, and to choose a current mode, for which there is a minimum ensuring the win in the refrigeration factor of up to 15 %. Increasing the value of the relative working current in the working range leads to a reduction in the time to enter a stationary mode by about 2 times, while the growth in temperature difference in the working range increases this indicator by about 2 times.

## References

- Zaykov, V. P., Kinshova, L. A., Moiseev, V. F. (2009). Prognozirovanie pokazateley nadezhnosti termoelektricheskikh ohlazhdayushchih ustroystv. Kniga 1. Odnokaskadnye ustroystva. Odessa: Politehperiodika, 120.
- Shalumova, N. A., Shalumov, A. S., Martynov, O. Yu., Bagayeva, T. A. (2011). Analysis and provision of thermal characteristics of radioelectronic facilities using the subsystem ASONIKA-T. Advances in modern radio electronics, 1, 42–49.

3. Sootsman, J. R., Chung, D. Y., Kanatzidis, M. G. (2009). New and Old Concepts in Thermoelectric Materials. *Angewandte Chemie International Edition*, 48 (46), 8616–8639. doi: <https://doi.org/10.1002/anie.200900598>
4. Choi, H.-S., Seo, W.-S., Choi, D.-K. (2011). Prediction of reliability on thermoelectric module through accelerated life test and Physics-of-failure. *Electronic Materials Letters*, 7 (3), 271–275. doi: <https://doi.org/10.1007/s13391-011-0917-x>
5. Eslami, M., Tajeddini, F., Etaati, N. (2018). Thermal analysis and optimization of a system for water harvesting from humid air using thermoelectric coolers. *Energy Conversion and Management*, 174, 417–429. doi: <https://doi.org/10.1016/j.enconman.2018.08.045>
6. Bakhtiaryfard, L., Chen, Y. S. (2014). Design and Analysis of a Thermoelectric Module to Improve the Operational Life. *Advances in Mechanical Engineering*, 7 (1), 152419. doi: <https://doi.org/10.1155/2014/152419>
7. Erturun, U., Mossi, K. (2012). A Feasibility Investigation on Improving Structural Integrity of Thermoelectric Modules With Varying Geometry. Volume 2: Mechanics and Behavior of Active Materials; Integrated System Design and Implementation; Bio-Inspired Materials and Systems; Energy Harvesting. doi: <https://doi.org/10.1115/smasis2012-8247>
8. Song, H., Song, K., Gao, C. (2019). Temperature and thermal stress around an elliptic functional defect in a thermoelectric material. *Mechanics of Materials*, 130, 58–64. doi: <https://doi.org/10.1016/j.mechmat.2019.01.008>
9. Manikandan, S., Kaushik, S. C., Yang, R. (2017). Modified pulse operation of thermoelectric coolers for building cooling applications. *Energy Conversion and Management*, 140, 145–156. doi: <https://doi.org/10.1016/j.enconman.2017.03.003>
10. Zaykov, V., Mescheryakov, V., Zhuravlov, Y. (2017). Analysis of the possibility to control the inertia of the thermoelectric cooler. *Eastern-European Journal of Enterprise Technologies*, 6 (8 (90)), 17–24. doi: <https://doi.org/10.15587/1729-4061.2017.116005>
11. Zaykov, V., Mescheryakov, V., Zhuravlov, Y., Mescheryakov, D. (2018). Analysis of dynamics and prediction of reliability indicators of a cooling thermoelement with the predefined geometry of branches. *Eastern-European Journal of Enterprise Technologies*, 5 (8 (95)), 41–51. doi: <https://doi.org/10.15587/1729-4061.2018.123890>
12. Zaikov, V., Meshcheryakov, V., Zhuravlov, Y. (2015). Selection of parameters combination of thermoelectric materials for development of high-reliability coolers. *Eastern-European Journal of Enterprise Technologies*, 3 (8 (75)), 4–14. doi: <https://doi.org/10.15587/1729-4061.2015.42474>